Design and Study of a Circular Polarised Conical-Disc-Backed Spiral Antenna for X-Band Applications

MASOOD UR-REHMAN[1], **(Senior Member, IEEE), GHAZANFAR ALI SAFDAR**[1],
XIAODONG YANG[2], **(Senior Member, IEEE), AND XIAODONG CHEN**[3], **(Fellow, IEEE)**

[1]School of Computer Science and Technology, University of Bedfordshire, Luton LU1 3JU, U.K.
[2]School of Electronic Engineering, Xidian University, Xi'an 710071, China
[3]School of Electronic Engineering and Computer Science, Queen Mary University of London, London E1 4NS, U.K.

Corresponding authors: Masood Ur-Rehman (masood.urrehman@beds.ac.uk) and Xiaodong Yang (xdyang@xidian.edu.cn)

ABSTRACT Design of a conical-disc-backed circular-polarized Archimedean single-arm spiral antenna is presented in this paper. The antenna operation covers the X-band frequencies ranging from 8 to 12 GHz. The antenna makes use of a very simple structure having the single-arm spiral backed by a cone-shaped metallic disc to achieve high gain, circular polarization, and unidirectional symmetric radiation near the boresight. The diameter of the antenna only measures to 40 mm. The simulated and measured results show that the antenna has a very good impedance matching (better than -10 dB), good right-hand circular polarization (with an axial ratio of ≤ 3 dB) throughout the frequency range of interest, and offers a maximum peak gain of 11.4 dBiC. The presented S_{11} response and radiation pattern results also show that the antenna offers excellent performance in the X-band with no need of a balun. Antenna usefulness is also established through a detailed parametric study and comparison with a traditional flat disc structure. Compact size, simple design, wide range, and high gain make the proposed antenna design a good choice for radar, terrestrial communications, and satellite/aerospace communications applications.

INDEX TERMS X-band, spiral antenna, high gain antenna, radar, terrestrial communications, satellite and aerospace communications, amateur radio.

I. INTRODUCTION

Demand of wireless communication devices is ever-growing. It has been predicted by the Wireless World Research Forum (WWRF) that 7 trillion wireless devices will serve 7 billion people by the end of this year [1]. IEEE Standard 521-2002 has assigned the electromagnetic spectrum ranging from 8 GHz to 12 GHz for X-band devices [2]. These frequencies are typically used for radar, satellite and terrestrial communications. A number of applications operate at these frequencies to deliver varying services including remote sensing, direction finding and surveillance and facilitate early warning, electronic counter-measures, telemetry, radar and flush mounted airborne systems [3].

Antenna plays the pivotal role in the performance of these wireless applications that mostly require high gain and circularly polarised antennas. Features like compact size, low profile, ease of integration, mechanical stability and simple

design are also desired for receiving terminals as well as the antenna mounted on the space segments and satellites [4]. Spiral antennas belong to the class of wide-band frequency independent antennas. They are inherently circular polarised and offer simple design, high gain and wide-beam operation [5], [6]. These features make them to efficiently fill aforementioned specifications and hence, a popular choice for the X-band applications.

Design of spiral antennas has attracted great interest from both the academia and industry recently. They are usually designed as a planar structure having an Archimedean, or logarithmic radiator in a circular, square or rectangular shape [5], [7], [8]. Different techniques and propositions are discussed by the researchers to achieve efficient spiral antenna designs meeting various specifications. Generally, the spiral antennas can be divided into four categories; spiral antennas in free space [5], [9], [10], spiral antennas

on planar reflectors [7], [8], [11], spiral antennas backed by cavities [12]–[14] and spiral antennas mounted on dielectric substrates [15], [16].

A combination of dielectric and inductive loading and ferrite-coated ground plane has been used by Kramer *et al.* to reduce the size of the spiral antenna [17]. Kashyap *et al.* have proposed using a two-arm Archimedean spiral loaded with two orthogonal dielectric slabs of FR-4 to improve the impedance bandwidth [18]. It increases the height of the antenna to become 67 mm. A slot spiral antenna loaded with ceramic materials having permittivities of more than 30 has been analysed for size reduction and low frequency operation in [12].

Afsar *et al.* have proposed a broadband spiral antenna having an Archimedean spiral at inner turn and an Archimedean spiral with a zigzag shape at outer turn [19]. An Archimedean spiral antenna consisting of two arms made of vertical metallic strips has been proposed by Guraliuc *et al.* [20]. This structure provides control of input impedance and polarisation purity by varying the strip width and turn thickness. The wide-band spiral antenna operation has been transformed into a dual-band operation by using a frequency-selective surface (FSS) as the ground plane by Chiu and Chuang [21]. Combination of a square spiral and a parasitic monopole printed on a double-sided RO4350B laminate has been used to aceive two distinct operating bands at 433 MHz and 2.45 GHz [22]. The antenna is fed through a grounded-coplanar-waveguide feedline.

Spiral antennas backed by metallic reflectors/discs offer high gain and directivity at the cost of decreased bandwidth [7]. Prevention of mutual coupling between the antenna and reflector to avoid deterioration in axial ratio is also a challenging task [23]. Cavity backed and reflector backed antennas can be easily mounted on metallic platforms and therefore, have attracted interest of researchers. Nakano *et al.* have presented a single-arm spiral antenna design with a small disc and backed by a cavity for ultra-wideband (UWB) operation [24]. A cavity-backed polygonal spiral antenna has been presented for UWB operation in [14]. A broadband, cavity-backed slot spiral antenna employing meandering in the outer turns has been proposed by Filipovic and Volakis [25] for efficient low band operation. A dual band operation at GPS L1 and L2 bands has been achieved by using a cavity-backed four-arm spiral antenna with asymmetric lengths in [26]. A four-arm Archimedean spiral antenna backed by a metallic reflector with a tapered transmission line feed has been presented by Li *et al.* for broadband operation at 0.8-3 GHz [27]. An FR-4 based hybrid antenna consisting of a two-arm spiral and meandered dipole for 868 MHz and 3.1-4.8 GHz bands has been discussed in [28].

Though having found good applicability in systems requiring CP operation at frequencies of 1-6 GHz, this attractive and useful antenna type has fewer design discussions for the X-band applications. Electromagnetic band-gap (EBG) structures are used to back the Archimedean spiral antennas by Bell and Iskander [29] to reduce the height of the antenna.

An equiangular spiral antenna is backed by an EBG reflector to achieve a unidirectional beam in the X-band frequency range in [30]. An Archimedean spiral consisting of a hybrid structure of backed-cavity with EBG and a perfect electrical conductor is proposed by Liu *et al.* [31] to increase the bandwidth. Parasitic loading of a PEC-backed equiangular spiral antenna using metallic posts has been employed by Veysi and Kamyab [32] to achieve size reduction and high bandwidth. The performance of the spiral with and without backing of a FSS reflector to suppress the backlobe radiation has been investigated in [33]. The ground plane presence in this antenna design affects the symmetry of the radiation pattern. Design of a wideband two-arm spiral antenna has been discussed by Liu *et al.* [34]. The antenna has a dome shape using liquid metal alloys encased into an inflated elastomer and can reconfigure the directivity.

Most of these spiral antenna solutions either have a broadband response or compact size but not both [24], [30]–[33]. Moreover, the structures are mechanically less stable and employs complex geometries limiting their applicability. Therefore, an investigative study by discussing a novel design of a compact and wideband spiral antenna for operation in X-band is presented in this work. The antenna makes use of a single-arm spiral structure backed by a cone-shaped metallic disc and covers frequencies from 7.26 GHz to 12.65 GHz. Evaluation of the antenna performance is analysed through numerical analysis and verified through measurements.

Following the introduction, this paper is organised in four sections. In Section II, description of the antenna design and working of the novel antenna through parametric study is elaborated. Section III presents the simulated and measured results of the proposed antenna structure. Section IV compares the performance of the proposed conical-disc-backed antenna with a flat-disc-backed antenna of similar geometry. This section also provides a comparison of the proposed antenna with state-of-the-art designs to establish its usefulness. Finally conclusions are drawn in Section V.

II. ANTENNA DESIGN AND INNOVATION
A. CONCEPT AND TOPOLOGY
X-band applications typically require wideband and high gain operation with circularly polarised propagation [4]. Simple geometry is also a preferred choice to reduce the complexity and associated cost. A spiral structure fits very well to meet these requirements as these antennas inherently offer wide bandwidth and circular polarisation. The presented antenna therefore, uses a simple single-arm Archimedean spiral geometry printed on a Rogers RO4350B substrate and fed using a 50 Ω unbalanced coaxial line. As compared to the two-arm design, this antenna has the advantage of being directly fed by the coaxial line without the need of a balun [35]. High gain and uni-directional radiation pattern is obtained through backing the spiral with a metallic disc. The disc is shaped in the form of a cone to reduce the radiation pattern tilt and improve its symmetry around the boresight.

An air-gap is used between the substrate and the cone-shaped disc to minimise mutual coupling and enhance axial ratio. The gap also contributes towards bandwidth improvements as explored in the parametric study in the following section (Fig. 3(a)) [24]. The structure offers strength in terms of mechanical stability and is therefore, good for mounting on metallic platforms.

The proposed antenna is modelled numerically and simulated using CST Microwave Studio® software package. The software uses the Finite Integration Technique (FIT) for the solution of Maxwell's equations [36]. The schematic layout of the modelled antenna structure is shown in Fig. 1.
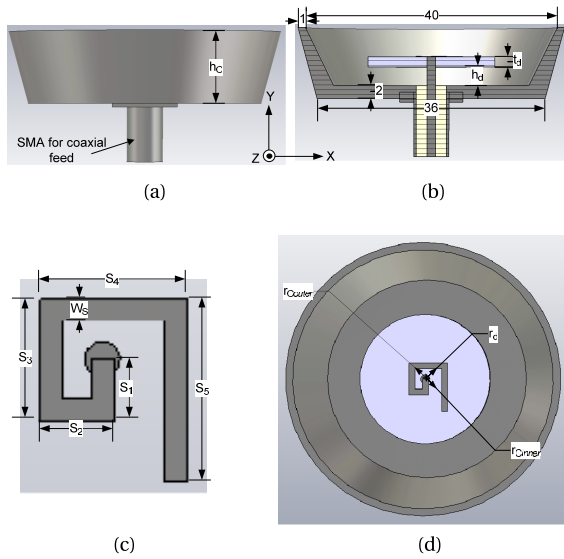

FIGURE 1. Schematic layout of the designed single-arm spiral antenna backed by a cone-shaped disc for X-band operation (all units are in mm). (a) Front view. (b) Cross-section view. (c) Spiral configuration. (d) Top view.

The proposed single-arm spiral antenna consists of five sections. For the centre frequency of 10 GHz, the total length of the spiral is chosen to be $0.8\lambda_{10} = 24mm$ (where λ_{10} represents the wavelength at 10 GHz) and it is calculated as:

$$S_{TOTAL} = S_1 + \sum_{i=2}^{i=5} A\left[log(i) - B\right]S_1 \qquad (1)$$

where, $S_1 = 0.082\lambda_{10} = 2.45mm$ is length of the first spiral section and S_i is lengths of the subsequent spiral sections. Values of A and B are chosen to be 2 and 0.1, respectively.

The cone-shaped metallic disc has an outer diameter of $1.34\lambda_{10} = 40mm$ and an inner diameter of $1\lambda_{10} = 30mm$. The height of the cone h_C is chosen to be 10 mm to serve two purposes; to improve the directivity and gain of the antenna, and bring symmetry to the radiated field. It also contributes towards the impedance bandwidth. The cone has a thickness of 2 mm at the bottom and 1 mm at the top edge.

The spiral radiator is printed on a single-sided Rogers RO4350B substrate of diameter $\frac{1}{3}\lambda_{10} = 10mm$. The substrate has a thickness of 1.524 mm, a relative permittivity of 3.6 and $tan\delta = 0.0031$. The gap between the substrate and the conical

TABLE 1. Optimised design parameters for the proposed single-arm spiral antenna for X-band operation.

Antenna Element	Parameter	Dimension (mm)
Cone-shaped disc	h_C	10
	$r_{C_{inner}}$	15.5
	$r_{C_{outer}}$	20
Dielectric substrate	r_d	11
	t_d	1.524
	h_d	2.9
	ϵ_r	3.6
Spiral	S_1	2.5
	S_2	2.9
	S_3	4.9
	S_4	6.3
	S_5	7.4
	W_S	0.9

disc, h_d, plays an important role in circular polarisation. earlier reports suggest that this gap should ideally be $\geq \frac{1}{4}\lambda$ for better circular polarisation [35]. We however, noted that for the proposed antenna, a higher axial ratio in the entire X-band can be achieved at a gap lower than the $\frac{1}{4}\lambda$. Its value is therefore, selected to be 2.9 mm to have better axial ratio along with improved bandwidth and gain. Use of the air gap between the conical disc and substrate helps to cope with the reverse current problem. Optimised antenna dimensions are given in Table 1.

The surface current distribution on the spiral antenna at 8 GHz, 10 GHz and 12 GHz is illustrated in Fig. 2(a), (b) and (c), respectively. The results show that the surface current is distributed alongside the spiral arm within the antenna surface. The current forms a travelling wave from the feed point to the edge of the spiral. Location of the highest current density along the spiral shifts with change in the frequency. The cone-shaped disc also collects some portions of the current and helps in obtaining a unidirectional and nearly symmetric radiation at the three frequencies by directing the wave in normal direction and maximising energy concentration axially.

B. PARAMETRIC STUDY
To enhance the understanding of the antenna operating principle, a detailed parametric study has been carried out considering effects of vital structural parameters on the antenna performance. Effects of the spiral width (W_S), cone height (h_C) and height of substrate (h_d) on the proposed antenna's S_{11}, -10 dB bandwidth, gain, axial ratio and field concentration (for directivity) are analysed. Results for S_{11} variations are compared in Fig. 3 while impact on the field strength is illustrated in Fig. 4. Observations on bandwidth, axial ratio and gain changes are summarised in Table 2.

It is observed that a decrease in the cone height improves the axial ratio at the expense of gain and bandwidth. A higher cone gives better gain due to improved directionality,
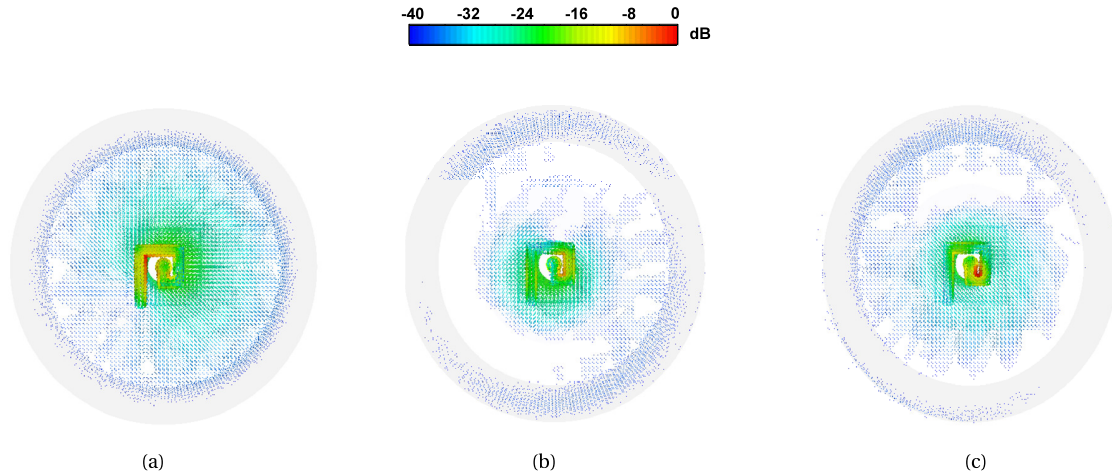
FIGURE 2. Surface current distribution on the proposed antenna at (a) 8 GHz, (b) 10 GHz and (c) 12 GHz.
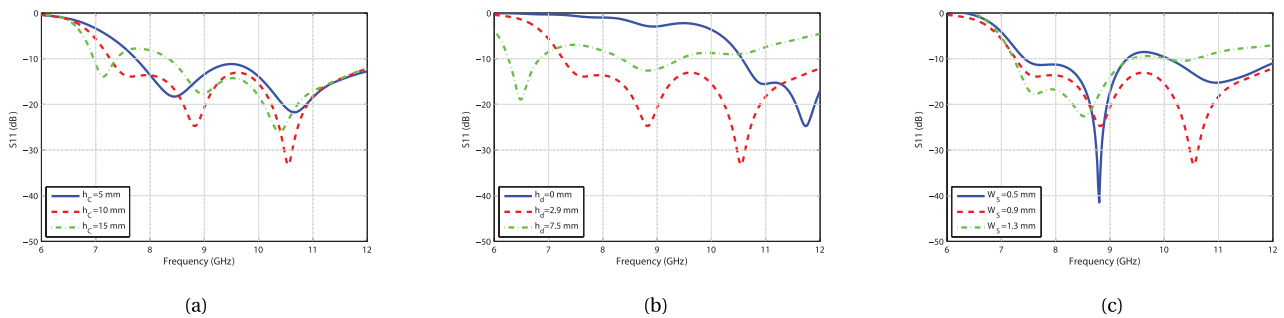

FIGURE 3. S_{11} variation for changing height of the cone-shaped disc, height of the substrate and width of the spiral arm on the performance of proposed X-band antenna. (a) Varying cone height. (b) Varying substrate height. (c) Varying spiral width.
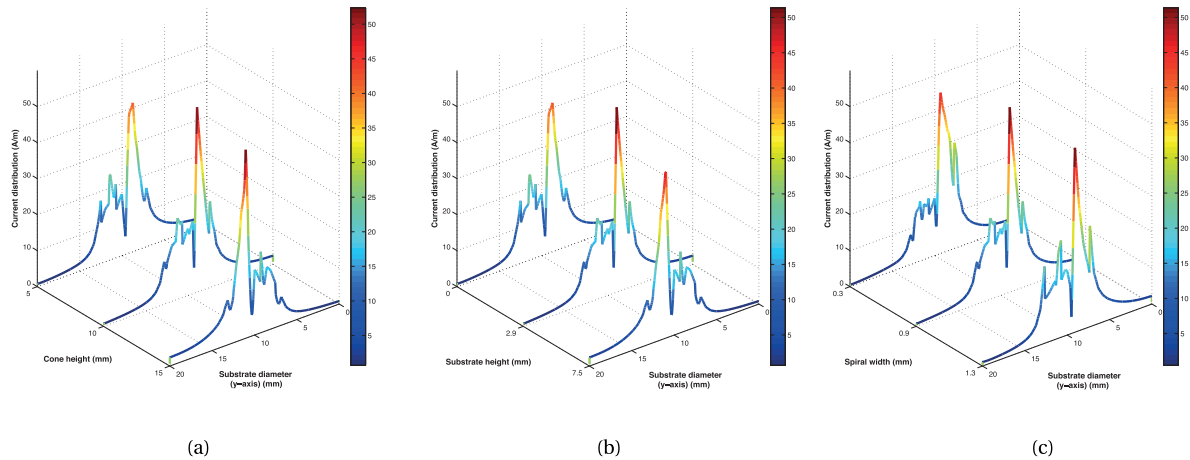

FIGURE 4. H-field variation along the diameter of the antenna at 10 GHz for varying height of the cone-shaped disc, height of the substrate and width of the spiral arm on the performance of proposed antenna. (a) Varying cone height. (b) Varying substrate height. (c) Varying spiral width.

however, axial ratio and bandwidth is reduced. Lower frequencies are more sensitive to any change in the cone height with a trend of upward shift. A decrease in the substrate height brings a reduction in all considered antenna parameters due to increased mutual coupling between the spiral and conical

disc. Increasing the substrate height tends to improve the axial ratio and gain caused by decrement in the mutual coupling due to higher air-gap but reduces the bandwidth. Gain at $h_d = 7.5 mm$ is nearly comparable (with a difference of 0.4 dB at two lower frequencies) to that being observed at

TABLE 2. Parametric study of proposed single-arm spiral antenna.

Antenna Property	Frequency (GHz)	Structural Parameter						
		Cone height (h_C)		Substrate height (h_d)		Spiral width (W_S)		Optimised
		5 mm	15 mm	0 mm	7.5 mm	0.3 mm	1.3 mm	h_C=10 mm h_d=2.6 mm W_S=0.9 mm
Bandwidth (GHz)	-	7.73-13.01	8.29-13.01	10.58-12.41	8.34-9.49	7.37-9.49, 9.94-12.55	7.15-11.08	7.26-12.65
Axial ratio (dB)	8	2.1	4.1	5.1	4.9	3.5	4.1	2.2
	10	1.6	3.2	8.5	3.9	7.0	2.6	1.8
	12	0.8	2.4	6.3	3.2	0.7	0.6	1.0
Gain (dBiC)	8	5.5	7.3	8.1	6.5	5.5	7.2	6.9
	10	8.1	11.2	10.4	10.5	10.1	11.1	10.9
	12	9.9	11.8	7.5	11.2	10.5	11.6	11.2

the optimised value of $h_d = 2.9mm$. Both lower and upper frequency bands are influenced with severe detuning and bandwidth reduction as a result of any change in the substrate height. A wider spiral arm gives higher gain as expected but reduces the axial ratio and bandwidth while a narrower spiral arm brings down gain, axial ratio and bandwidth. Changing the value of this parameter significantly reduces the antenna impedance matching and detunes it due to perturbing current distribution along the spiral and shifting the location of the current maxima. It is also noted that although affected by all of the three parameters, impedance matching depends greatly on the height of the substrate from the disc and hence the air-gap.

The ability of the antenna to concentrate the field along the boresight increases with an increase in the cone height due to reduced current spreading as shown in Fig. 4(a). This improvement of 1 A/m is however, not significant due to higher impedance mismatch and losses. A decrease in the substrate height reduces the field concentration due to increased level of reverse currents as shown in Fig. 4(b). Field concentration for the increased substrate height is comparable to that observed for the reduced height as this configuration causes a reduced cone height. The change in the spiral width also impacts the level of field concentration. Less wider spiral reduces the field concentration due to smaller cross sectional area. A wider spiral tends to increase the field concentration but only attains a level comparable to the opti-mised values due to impedance mismatch losses as illustrated in Fig. 4(c).

The antenna dimensions, therefore, need to be selected carefully in order to balance the tradeoff between the three parameters and maximise its performance. It appears that optimised values of h_C, h_d and W_S is a good choice to have higher gain, good axial ratio in the direction of maximum radiation, wider bandwidth and more concentrated field near the boresight. Although, the optimised antenna dimensions slightly reduces the axial ratio, it remains below the required threshold of 3 dB.

(a)   (b)
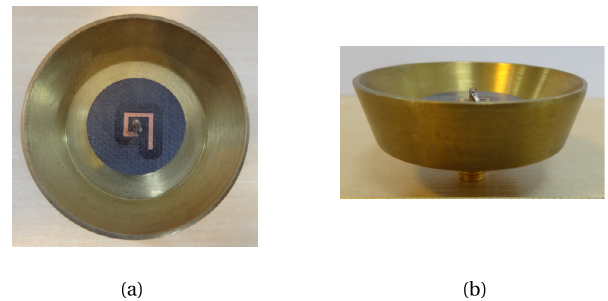
FIGURE 5. Fabricated prototype of the proposed X-band antenna. (a) Top view. (b) Side view.

III. ANTENNA FABRICATION AND MEASUREMENTS

In order to verify the proposed design, a prototype of the antenna is fabricated and tested. The fabricated antenna is shown in Fig. 5. The impedance and radiation characteristics of the proposed X-band antenna are then evaluated through-out the range of the operating frequencies through measure-ments in an anechoic chamber using Agilent's HP8720ES Vector Network Analyser (VNA). In order to mitigate the cable effects, ferrite beads have been used. The measured results are compared with the simulations to validate the experiment.

Comparison of the simulated and measured S_{11} responses of the proposed X-band antenna in free space is given in Fig. 6. The simulated results agree very well with the mea-surements. The antenna achieves a -10 dB impedance band-width of 5.4 GHz in simulation (ranging from 7.26 GHz to 12.65 GHz) and 5.1 GHz in measurement (ranging from 7.25 GHz to 12.35 GHz) and effectively covers all the fre-quencies required for the X-band operation. Small discrepan-cies present between the two results are most likely associated to the fabrication tolerances.

Fig. 7 presents the comparison of the simulated and mea-sured radiation patterns at 8 GHz, 10 GHz, and 12 GHz, respectively. The simulated radiation patterns are in good
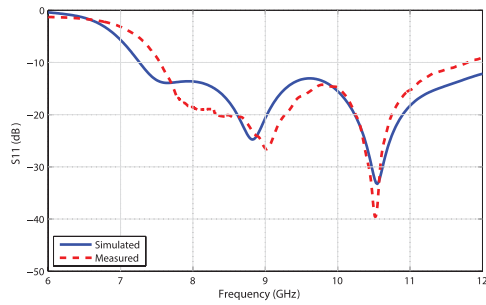
FIGURE 6. Simulated and measured S_{11} response of the proposed single-arm spiral antenna.

agreement with the measurements across the band of interest. Distortions in the back lobes of the measured plots are due to the reflected currents flowing on the outer conductor of the feeding cable in this balun-free structure. The presence of the SMA connector in the fabricated prototype also contributes towards it. Overall, the antenna exhibits good radiation coverage throughout the X-band frequency range. The antenna radiates one wide major lobe and small back lobes with a front-to-back ratio of ≤ 20 dB. It efficiently covers the upper hemisphere which is necessary for the satellite communications. The E_θ and E_ϕ components are nearly the same making the antenna to obtain good circular polarisation. The cone-shaped disc also significantly mitigates the asymmetric radiation about the boresight throughout the operating band that is a common degradation suffered by the reflector-backed spiral antennas.

The axial ratio is calculated using:

$$AR = \frac{|E_R| + |E_L|}{|E_R| - |E_L|} \quad (2)$$

where,

$$E_R = \frac{1}{\sqrt{2}}\left(E_\theta + jE_\phi\right) \quad (3)$$

and

$$E_L = \frac{1}{\sqrt{2}}\left(E_\theta - jE_\phi\right) \quad (4)$$

E_θ and E_ϕ represent the components of the radiated electric field. Fig. 8(a) presents the comparison of simulated and measured axial ratio results of the proposed X-band antenna along the direction of maximum radiation. The results show that the antenna efficiently achieves the 3-dB axial ratio in the whole of the X-band region of 8 GHz to 12 GHz. Minimum axial ratio is 1.0 dB at 12 GHz in simulation and 1.3 dB at 11 GHz in measurement while its maximum value is 2.5 dB at 11 GHz in simulation and 1.8 dB at 8 GHz in measurement. Overall, a very good circular polarisation bandwidth is expressed by the antenna both in simulation and measurement.

The simulated and measured peak gain values are plotted in Fig. 8(b). The antenna gain performance in simulation is well-consistent with those of the measured gains. It is evident from these results that the antenna offers very good gain performance in the required frequency band reaching a maximum value of 11.2 dBiC in simulation and 11.4 dBiC in measurement at 12 GHz. Antenna gain in the X-band region
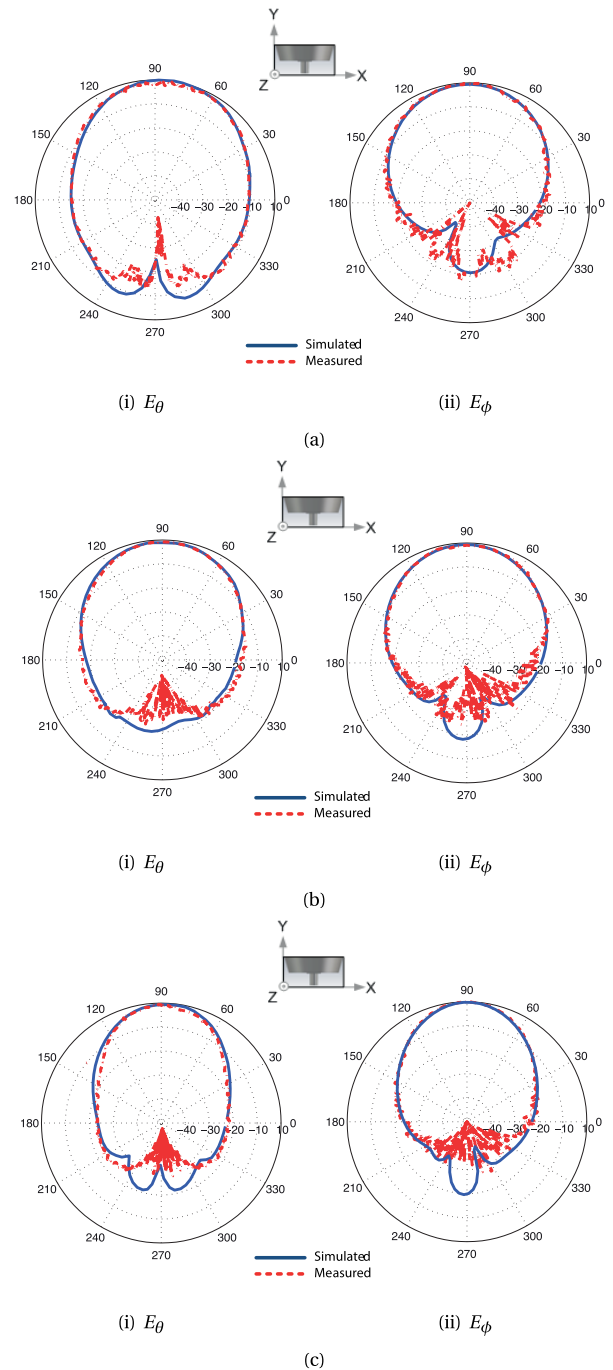

FIGURE 7. Simulated and measured radiation patterns of proposed single-arm spiral antenna at 8 GHz, 10 GHz and 12 GHz. (a) $f = 8GHz$. (b) $f = 10GHz$. (c) $f = 12GHz$.

is observed to be minimum at 8 GHz as the antenna has wider beamwidth and less focused radiation along the boresight due to current spreading. It ultimately reduces the gain as compared to the two higher frequencies where antenna achieves higher directivity. The observation of the current distribution and radiation pattern in Figs. 2 and 7 further confirm it. The aperture efficiency of the antenna is calculated and found to be 36%, 60% and 66% at 8, 10 and 12 GHz, respectively. The proposed antenna offers good efficiency at the two higher
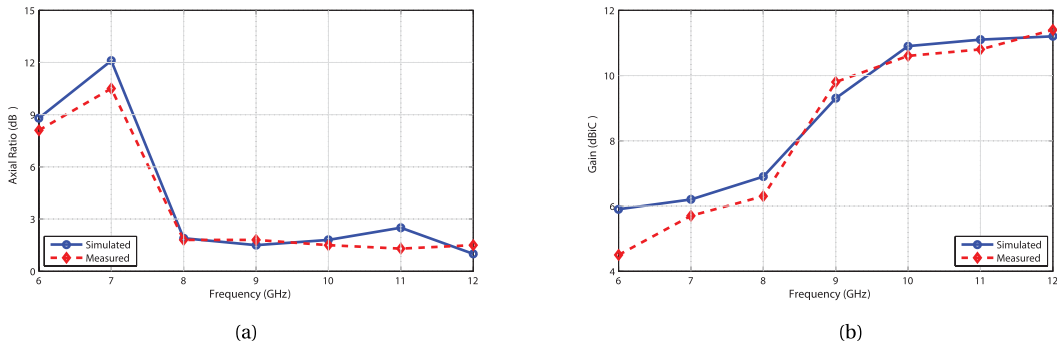
(a)   (b)

FIGURE 8. Simulated and measured values of axial ratio in the maximum radiation direction and maximum gain of the proposed single-arm spiral antenna. (a) Axial ratio. (b) Gain.
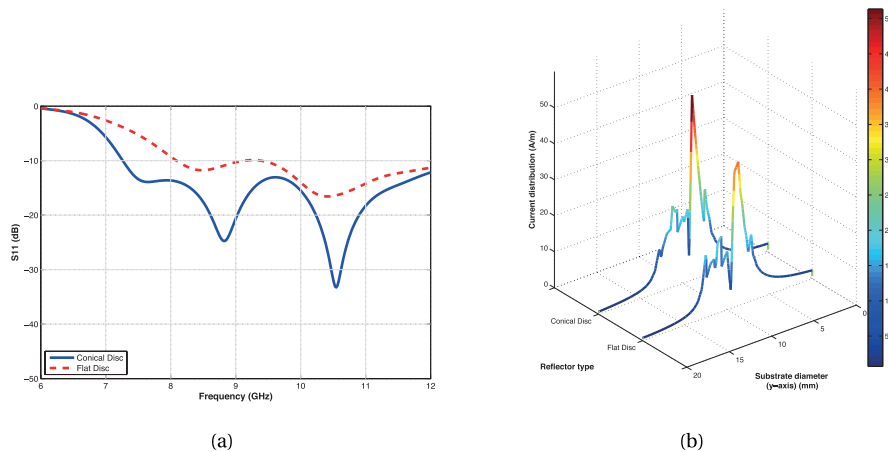

(a)   (b)

FIGURE 9. Comparison of S_{11} response and H-field variation along the diameter of the antenna for the proposed antenna with cone-shaped disc and flat disc. (a) S_{11} response. (b) Field distribution.

frequencies while efficiency at 8 GHz is acceptable. It also shows that more losses take place at 8 GHz contributing to a lower gain value.

IV. COMPARISON AND DISCUSSION

A. SINGLE ARM SPIRAL WITH FLAT DISC

In order to show the effectiveness of the proposed single-arm spiral antenna backed by a cone-shaped disc over the traditional flat disc structure, the antenna with flat disc is also studied numerically. The antenna carries the same dimensions except the shape of the disc. A comparison between the two configurations in terms of S_{11}, radiation pattern, bandwidth, axial ratio, maximum gain, direction of maximum radiation, 3 dB beamwidth and field concentration is made and presented in Figs. 9 and 10 and Table 3.

Fig. 9(a) compares the S_{11} response of the two configurations. The antenna with flat disc shows poor impedance matching with a detuned operation at the lower frequency band. The lower band undergoes an upward shift loosing 0.75 GHz of the band. These results are in line with the previous discussion and confirms that the cone height contributes towards the bandwidth on top of axial ratio and gain. The conical-disc also helps the antenna to focus the

field (Fig. 9(b)) and hence, achieve a higher gain and more directional beamwidth. In comparison to a maximum of 11.2 dBiC gain of the proposed antenna, flat disc configuration exhibits a maximum value of 7.7 dBiC due to wider and tilted beamwidth.

Radiation patterns for the two antennas at 8 GHz, 10 GHz and 12 GHz are compared and illustrated in Fig. 10. It is evident from these plots that though having a similar radiation profile, the antenna with the flat disc radiates a tilted beam well in accord with earlier reported studies. The proposed antenna with conical-disc overcomes this issue effectively by having a nice symmetrical radiation pattern around the boresight in upper hemisphere throughout the X-band. It is further confirmed by observing the maximum radiation direction which is close to 90° at the three studied frequencies. The flat disc, on the other hand, tilts the maximum radiation by a minimum of 20°.

These results show that the proposed antenna geometry has clear advantages of higher gain, symmetric pattern and focused radiation. The flat disc, however, has a slight edge in terms of axial ratio but the obtained values are nearly comparable with maximum difference of 0.3 dB at 8 GHz.

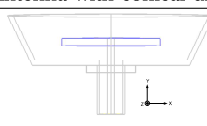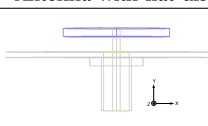**TABLE 3.** Comparison between the proposed antenna having a cone-shaped disc and the antenna having a flat disc.

Antenna Property	Frequency (GHz)	Antenna Type	
		Antenna with conical disc	Antenna with flat disc
Bandwidth (GHz)	-	7.26-12.65	8.2-12.1
Axial ratio (dB)	8	1.9	2.5
	10	1.8	1.9
	12	1.0	0.6
Gain (dBiC)	8	6.9	4.4
	10	10.9	6.8
	12	11.2	7.7
Maximum radiation direction	8	$E_\theta = 80°$ $E_\phi = 88°$	$E_\theta = 60°$ $E_\phi = 70°$
	10	$E_\theta = 91°$ $E_\phi = 87°$	$E_\theta = 113°$ $E_\phi = 110°$
	12	$E_\theta = 88°$ $E_\phi = 90°$	$E_\theta = 63°$ $E_\phi = 114°$
3 dB beamwidth	8	$E_\theta = 52°$ $E_\phi = 59°$	$E_\theta = 132°$ $E_\phi = 75°$
	10	$E_\theta = 49°$ $E_\phi = 49°$	$E_\theta = 71°$ $E_\phi = 73°$
	12	$E_\theta = 45°$ $E_\phi = 42°$	$E_\theta = 99°$ $E_\phi = 80°$

TABLE 4. Comparison between the proposed antenna and reported spiral antennas for X-band operation.

Ref.	Antenna structure	Size	BW in X-band	Max. axial ratio in X-band (dB)	Gain (dBiC)
[24]	Single circular spiral backed by conducting disc and cavity	$0.8\lambda \times 0.07\lambda$	50%	0.8	7.5
[29]	EBG backed dual arm spiral	$1.1\lambda \times 1.1\lambda \times 0.02\lambda$	42.5%	Not reported	9.0
[30]	EBG backed equiangular spiral	$2.5\lambda \times 2.5\lambda \times 0.12\lambda$	25%	1.8	7.5
[31]	Hybrid (EBG+PEC) cavity backed dual arm spiral	$0.31\lambda \times 0.02\lambda$	50%	1.8	7.5
[32]	PEC reflector backed equiangular spiral with metallic posts	$1.8\lambda \times 1.8\lambda \times 0.1\lambda$	50%	5	6.2
[34]	Two arm liquid metal spiral encased into stretchable elastomer	$0.84\lambda \times 0.51\lambda$ (fully inflated)	100%	1.32	9.9
This work	Conical-disc-backed single arm spiral on FR-4	$0.9\lambda \times 0.2\lambda$	100%	1.8	11.4

B. REPORTED X-BAND SPIRAL ANTENNAS

Table 4 presents a comparison between the proposed antenna and state-of-the-art spiral antenna designs for X-band operation reported in open literature [24], [29]–[32], [34]. Size is calculated considering lowest operating frequency reported in these studies. The comparison show that the proposed antenna exhibits broader bandwidth for the coverage of the X-band operation between 8-12 GHz frequencies than all of the reported designs except presented in [34]. The proposed design also achieves the largest gain while axial ratio is comparable to [30] and [31] and better than [29] and [32]. It also has an overall smaller size as compared to [29], [30], [32], and [34] and lower profile. Compared to [24], Nakano et al. have used a circular spiral geometry in their single arm
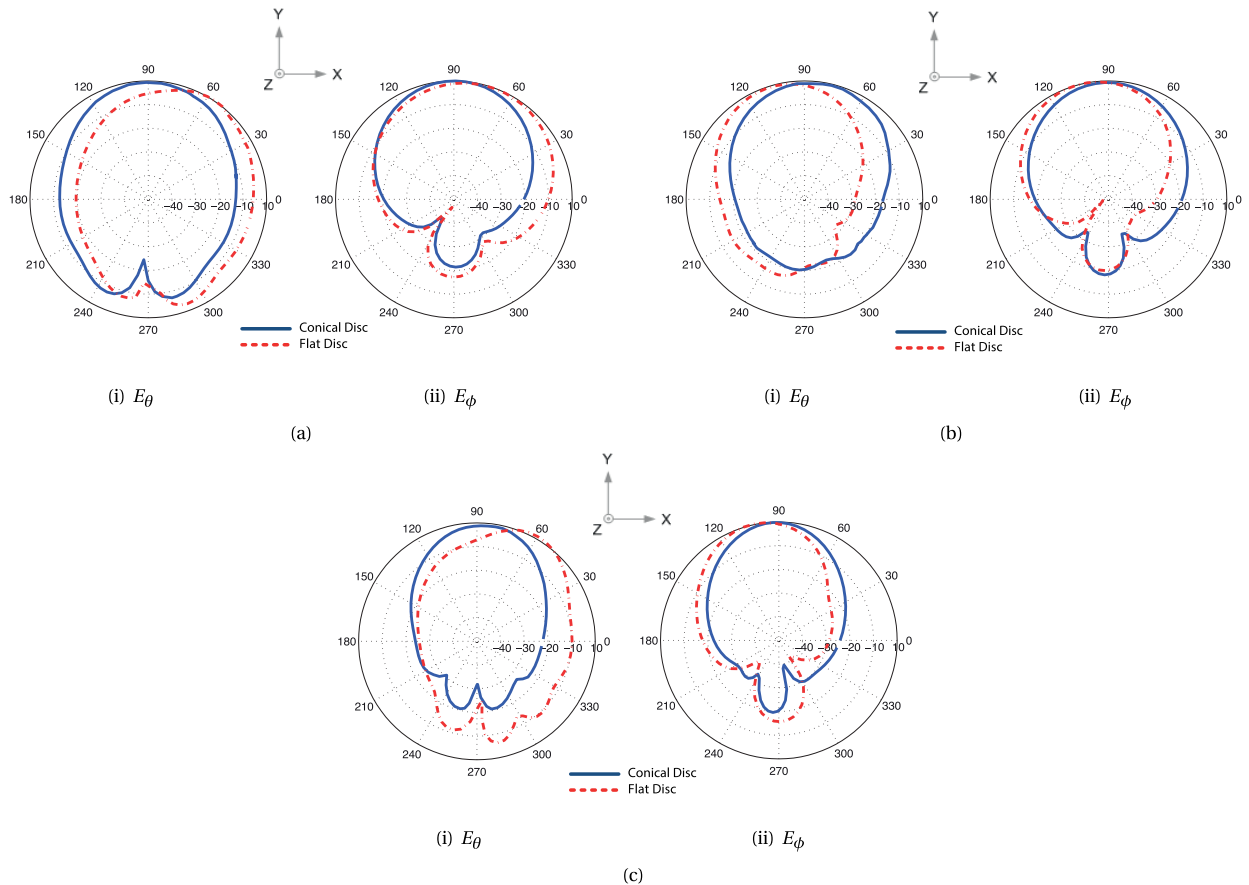
FIGURE 10. Comparison of radiation patterns of proposed antenna with cone-shaped disc and flat disc at 8 GHz, 10 GHz and 12 GHz. (a) $f = 8GHz$. (b) $f = 10GHz$. (c) $f = 12GHz$.

spiral (SAS) design with circumference of 213.6 mm. Their SAS is backed by a conducting disc (flat- reflector) and cavity. Size of this antenna is almost double the size of our proposed design having a cavity diameter of 80 mm. They have also used an absorbing material to reduce the reflected current. It operates in a frequency range of 3-10 GHz covering only the first half (8-10 GHz) of the X-band and the antenna gain is also lower than the proposed design as maximum gain in 8-10 GHz range is 7.5 dBiC. More importantly, unlike these designs, the proposed antenna has a simple geometry and can be fabricated using low cost traditional fabrication techniques. In addition, it supports a symmetrical radiation pattern along the boresight.

V. CONCLUSION

A novel spiral antenna backed by a cone-shaped disc for the wireless devices working in X-band has been proposed. The simulated results are verified and validated through measurements of the fabricated prototype. The proposed antenna offers small size and simple structure. The presented results show that the the proposed antenna covers the X-band frequencies of 8 GHz to 12 GHz with good 3 dB axial ratio and a maximum gain of 11.4 dBiC. It has been shown through a detailed parametric study that the antenna operation

depends primarily upon the height of substrate and height of cone. The proposed spiral antenna backed by the cone-shaped disc has also been compared with a configuration backed by a flat disc to establish its merits. The proposed design has successfully achieved a symmetric radiation pattern along the boresight with a focused beam effectively mitigating the radiation pattern degradations associated with flat-surface reflectors by making use of the cone-shaped disc. Though, a better axial ratio is achievable by using lower height of the conical-disc, the proposed antenna is a good compromise between the three vital parameters of gain, axial ratio and bandwidth. Consequently, this low profile antenna can be a promising candidate for radar, terrestrial, satellite and aerospace communication systems.

REFERENCES

[1] L. Sorensen and K. Skouby. (Jul. 2009). *User Scenarios 2020-a World-wide Wireless Future, WWRF*. [Online]. Available: http://www.wwrf.ch/files/publications
[2] *IEEE Standard Letter Designations for Radar-Frequency Bands*, IEEE Standards I. S. 521-2002, Jan. 2003.
[3] M. Richaria, *Satellite Communications Systems*. London, U.K.: McGraw-Hill, 1999.
[4] T. Kitsuregawa, *Advanced Technology in Satellite Communication Antennas: Electrical and Mechanical Design*. New York, NY, USA: Artech House, 1990.

[5] W. Curtis, "Spiral antennas," *IRE Trans. Antennas Propag.*, vol. 8, no. 3, pp. 298–306, May 1960.

[6] J. Dyson, "The equiangular spiral antenna," *IRE Trans. Antennas Propag.*, vol. 7, no. 2, pp. 181–187, Apr. 1959.

[7] H. Nakano, K. Nogami, S. Arai, H. Mimaki, and J. Yamauchi, "A spiral antenna backed by a conducting plane reflector," *IEEE Trans. Antennas Propag.*, vol. AP-34, no. 6, pp. 791–796, Jun. 1986.

[8] J. J. H. Wang and V. K. Tripp, "Design of multioctave spiral-mode microstrip antennas," *IEEE Trans. Antennas Propag.*, vol. 39, no. 3, pp. 332–335, Mar. 1991.

[9] J. Kaiser, "The Archimedean two-wire spiral antenna," *IRE Trans. Antennas Propag.*, vol. 8, no. 3, pp. 312–323, May 1960.

[10] R. T. Gloutak and N. G. Alexopoulous, "Two-arm eccentric spiral antenna," *IEEE Trans. Antennas Propag.*, vol. 45, no. 4, pp. 723–730, Apr. 1997.

[11] M. Ur-Rehman, Q. H. Abbasi, M. Kamran, and X. Yang, "Design of a compact wearable single-arm spiral antenna for satellite communications," in *Proc. IEEE Int. RF Microw. Conf. (RFM)*, Dec. 2013, pp. 318–321.

[12] B. A. Kramer, M. Lee, C.-C. Chen, and J. L. Volakis, "Design and performance of an ultrawide-band ceramic-loaded slot antenna," *IEEE Trans. Antennas Propag.*, vol. 53, no. 7, pp. 2193–2199, Jul. 2005.

[13] J. L. Volakis, M. W. Nurnberger, and D. S. Filipovic, "Slot spiral antenna," *IEEE Antennas Propag. Mag.*, vol. 43, no. 6, pp. 15–26, Dec. 2001.

[14] N. Rahman and M. N. Afsar, "A novel modified archimedean polygonal spiral antenna," *IEEE Trans. Antennas Propag.*, vol. 61, no. 1, pp. 54–61, Jan. 2013.

[15] H. Nakano, M. Ikeda, K. Hitosugi, and J. Yamauchi, "A spiral antenna sandwiched by dielectric layers," *IEEE Trans. Antennas Propag.*, vol. 52, no. 6, pp. 1417–1423, Jun. 2004.

[16] C. Penney and R. J. Luebbers, "Input impedance, radiation pattern, and radar cross section of spiral antennas using FDTD," *IEEE Trans. Antennas Propag.*, vol. 42, no. 9, pp. 1328–1332, Sep. 1994.

[17] B. A. Kramer, C.-C. Chen, and J. L. Volakis, "Size reduction of a low-profile spiral antenna using inductive and dielectric loading," *IEEE Antennas Wireless Propag. Lett.*, vol. 7, pp. 22–25, 2008.

[18] N. Kashyap and D. K. Vishwakarma, "Cross-dielectric-slab-loaded archimedean spiral antenna," *IEEE Antennas Wireless Propag. Lett.*, vol. 15, pp. 589–592, 2016.

[19] M. N. Afsar, Y. Wang, and R. Cheung, "Analysis and measurement of a broadband spiral antenna," *IEEE Antennas Propag. Mag.*, vol. 46, no. 1, pp. 59–64, Feb. 2004.

[20] A. Guraliuc, R. Caso, P. Nepa, and J. Volakis, "Numerical analysis of a wideband thick archimedean spiral antenna," *IEEE Antennas Wireless Propag. Lett.*, vol. 11, pp. 168–171, 2012.

[21] C.-N. Chiu and W.-H. Chuang, "A novel dual-band spiral antenna for a satellite and terrestrial communication system," *IEEE Antennas Wireless Propag. Lett.*, vol. 8, pp. 624–626, 2009.

[22] J. L. Buckley, K. G. McCarthy, L. Loizou, B. O'Flynn, and C. O'Mathuna, "A dual-ISM-band antenna of small size using a spiral structure with parasitic element," *IEEE Antennas Wireless Propag. Lett.*, vol. 15, pp. 630–633, 2016.

[23] T. Y. Shih and N. Behdad, "A compact, broadband spiral antenna with unidirectional circularly polarized radiation patterns," *IEEE Trans. Antennas Propag.*, vol. 63, no. 6, pp. 2776–2781, Jun. 2015.

[24] H. Nakano, R. Satake, and J. Yamauchi, "Extremely low-profile, single-arm, wideband spiral antenna radiating a circularly polarized wave," *IEEE Trans. Antennas Propag.*, vol. 58, no. 5, pp. 1511–1520, May 2010.

[25] D. S. Filipovic and J. L. Volakis, "Broadband meanderline slot spiral antenna," *IEE Proc.-Microw., Antennas Propag.*, vol. 149, no. 2, pp. 98–105, Apr. 2002.

[26] S. X. Ta and I. Park, "Dual-band operation of a circularly polarized four-arm curl antenna with asymmetric arm length," *Int. J. Antennas Propag.*, vol. 2016, Dec. 2015, Art. no. 3531089. [Online]. Available: https://www.hindawi.com/journals/ijap/2016/3531089/cta/

[27] D. Li, L. Li, Z. Li, and G. Ou, "Four-arm spiral antenna FED by tapered transmission line," *IEEE Antennas Wireless Propag. Lett.*, vol. 16, pp. 62–65, 2017.

[28] M. Fantuzzi, D. Masotti, and A. Costanzo, "A novel integrated UWB-UHF one-port antenna for localization and energy harvesting," *IEEE Trans. Antennas Propag.*, vol. 63, no. 9, pp. 3839–3848, Sep. 2015.

[29] J. M. Bell and M. F. Iskander, "A low-profile Archimedean spiral antenna using an EBG ground plane," *IEEE Antennas Wireless Propag. Lett.*, vol. 3, no. 1, pp. 223–226, Dec. 2004.

[30] H. Nakano, K. Kikkawa, N. Kondo, Y. Iitsuka, and J. Yamauchi, "Low-profile equiangular spiral antenna backed by an EBG reflector," *IEEE Trans. Antennas Propag.*, vol. 57, no. 5, pp. 1309–1318, May 2009.

[31] C. Liu, Y. Lu, C. Du, J. Cui, and X. Shen, "The broadband spiral antenna design based on hybrid backed-cavity," *IEEE Trans. Antennas Propag.*, vol. 58, no. 6, pp. 1876–1882, Jun. 2010.

[32] M. Veysi and M. Kamyab, "Bandwidth enhancement of low-profile PEC-backed equiangular spiral antennas incorporating metallic posts," *IEEE Trans. Antennas Propag.*, vol. 59, no. 11, pp. 4315–4318, Nov. 2011.

[33] S. Mohamad, R. Cahill, and V. Fusco, "Performance of archimedean spiral antenna backed by FSS reflector," *Electron. Lett.*, vol. 51, no. 1, pp. 14–16, 2015.

[34] P. Liu, S. Yang, X. Wang, M. Yang, J. Song, and L. Dong, "Directivity-reconfigurable wideband two-arm spiral antenna," *IEEE Antennas Wireless Propag. Lett.*, vol. 16, pp. 66–69, 2017.

[35] H. Nakano, J. Eto, Y. Okabe, and J. Yamauchi, "Tilted- and axial-beam formation by a single-arm rectangular spiral antenna with compact dielectric substrate and conducting plane," *IEEE Trans. Antennas Propag.*, vol. 50, no. 1, pp. 17–24, Jan. 2002.

[36] *CST Microwave Studio User Manual*, Comput. Simul. Technol. GmbH, Darmstadt, Germany, 2017.

MASOOD UR-REHMAN (SM'16) received the B.Sc. degree in electronics and telecommunication engineering from the University of Engineering and Technology, Lahore, Pakistan, in 2004, and the M.Sc. and Ph.D. degrees in electronic engineering from the Queen Mary University of London, London, U.K., in 2006 and 2010, respectively. He was with the Queen Mary University of London as a Post-Doctoral Research Assistant until 2012. He joined the Centre for Wireless Research at the University of Bedfordshire, Luton, U.K., as a Lecturer. He has been involved in a number of projects supported by industrial partners and research councils. He has contributed to a patent and authored/co-authored four books, seven book chapters, and over 75 technical articles in leading journals and peer-reviewed conferences. His research interests include compact antenna design, radiowave propagation and channel characterization, satellite navigation system antennas in cluttered environment, electromagnetic wave interaction with human body, body-centric wireless networks and sensors, remote health care technology, mmWave and nano-communications for body-centric networks, and D2D/H2H communications.

Dr. Ur Rehman is a fellow of the Higher Education Academy (U.K.), a member of IET and part of the technical program committees and organizing committees of several international conferences, workshops, and special sessions. He is an Associate Editor of the IEEE Access and lead guest editor of numerous special issues of renowned journals. He also serves as a reviewer for book publishers, the IEEE conferences, and leading journals.

GHAZANFAR ALI SAFDAR received the B.Sc. degree (Hons.) in electrical engineering from the University of Engineering and Technology, Pakistan, the M.Eng. degree in computer science and telecommunications from ENSIMAG, INPG, France, and the Ph.D. degree from Queen's University Belfast, U.K., in 2005, with a focus on the area of power-saving MAC protocols for the IEEE 802.11 family of wireless LANs. He was a Research Fellow with Queen's University Belfast on a project related to wireless networks security funded by EPSRC Grant. He was a Research and Development Engineer with Carrier Telephone Industries (SIEMENS), Pakistan, and with Schlumberger, France. He is currently a Senior Lecturer in computer networking with the University of Bedfordshire, U.K. His research interests mainly include cognitive radio networks, energy saving MAC protocols, security protocols for wireless networks, LTE networks, interference mitigation, device-to-device communications, network modeling, and performance analysis. He is the General Chair of the 4th EAI GreeNets and serving as the Editor-in-Chief of the *EAI Transactions on Energy Web*.

XIAODONG YANG (SM'17) has authored over 30 peer-reviewed journal papers, including some IEEE transactions. He has a global collaborative research network in the field of antennas and propagation, wireless communications, health informatics, information security, microwave techniques, and Internet of Things. His research interests include body area networks, antennas and propagation, 5G, information security, wireless sensing, radar, millimeter wave technology, THz technology, nano-communications, biomedical nano-imaging, biomedical communications, visible light communications, and machine learning. He received the Young Scientist Award from the International Union of Radio Science in 2014. He is an active Reviewer of the IEEE Transactions on Antennas and Propagation, the IEEE Transactions on Microwave Theory and Techniques, the IEEE Antennas and Wireless Propagation Letters, the *IET Microwaves, Antennas & Propagation*, the IEEE Access Journal, and *Neurocomputing* (Elsevier).

XIAODONG CHEN (SM'96–F'16) received the B.Sc. degree in electronic engineering from the University of Zhejiang, Hangzhou, China, in 1983, and the Ph.D. degree in microwave electronics from the University of Electronic Science and Technology of China, Chengdu, in 1988. In 1988, he joined the Department of Electronic Engineering, King's College, University of London, as a Post-Doctoral Visiting Fellow. In 1990, he was a Research Associate with the King's College London and was appointed to an EEV Lectureship. In 1999, he joined the Department of Electronic Engineering, Queen Mary University of London, where he is currently a Professor. He has authored or co-authored over 300 publications (book chapters, journal papers, and refereed conference presentations). His research interests are in the fields of wireless communications, microwave devices, and antennas. He is currently a member of the U.K. EPSRC Review College and a Technical Panel of the IET Antennas and Propagation Professional Network.

• • •